Rapid Response All-Fiber Moisture Sensor

Jiamin Wang, Jiqiang Wang, Zhen Li, Zikun Yu, Shuo Li, Tongyu Liu, Tong Sun, and Kenneth T. V. Grattan

***Abstract*—Combining the benefits of photothermal conversion in a doped optical fiber with the principle of Fiber Bragg Grating (FBG)-based temperature measurement, a new optical fiber method for the measurement of moisture content has been developed and its performance is reported. This novel all-fiber approach shows the important characteristics of fast response, miniaturization in the design and low power consumption. In this work, a 1480nm pump laser has been used to heat the cobalt-doped fiber used, which has been embedded in the sample under investigation, where the sensor temperature change was obtained by using a FBG written into the cobalt-doped fiber. The fast, *in-situ* measurement of moisture content developed takes advantage of the linear relationship between the temperature change characteristics experienced during the heating process and the moisture content. To calibrate and characterize the sensor developed, a variable moisture-content test platform was established, and experiments were conducted to investigate the performance of this optical fiber approach. The all-fiber moisture sensor developed in this way has been evaluated by measuring the moisture content of samples of soil and pulverized coal and the data obtained were in good agreement with the results obtained from using the more conventional (and slow) drying method, with a maximum error of just over 1% and a rapid, 2s, optimum measurement time achieved.**

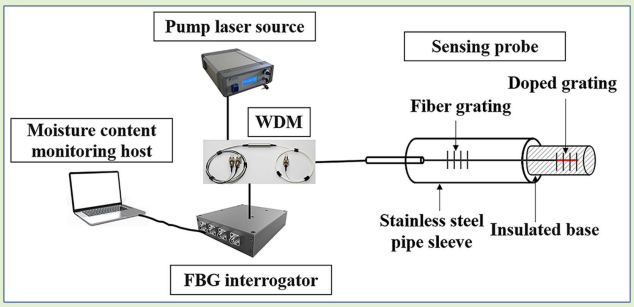

***Index Terms*—Moisture content, fast response, photothermal conversion, temperature characteristic value.**

I. Introduction

THE change of moisture content in the soil is one of the major factors which causes natural disasters such as landslides [1], the unwanted flow of industrial debris or other waste products [2] and results in flooding washing away a wide range of materials [3], causing danger to infrastructure and, frequently, loss of life. In order to provide warning of such incidents and to alert those who may be in danger before they happen, accurate monitoring of the change in moisture content of soils and other materials is important – in that way to avoid potentially heavy casualties and significant economic losses. At the same time, a good knowledge of the moisture content is also an important influencing factor for the better evaluation of the ground conditions in geotechnical engineering [4], in agricultural precision irrigation [5], and in hydrological condition research [6]. In particular, better real-time dynamic monitoring of moisture content can improve the utilization rate of water resources and agricultural crop yields, which will make better use of scarce resources and help protect the earth's ecological environment. In industries such as mining, the chemical industry, metallurgy and pharmacy, the accurate control of moisture content is used to ensure safety in production and to give better product quality control [7].

Currently, there are many different methods that can be used to measure moisture content. For example, the drying method which can be routinely used is destructive to the structure of the sample itself, and measurements can take a long time to perform. It is also essentially a laboratory-based measurement (and therefore subject to errors that may arise due to the time between sampling and the testing actually being carried out) and often is used for the calibration of other measurement methods [8]. Other techniques may also be problematic, for example the time domain reflection method can easily be disturbed when in use, is complex and overall is expensive to implement [9]. The tensiometer method has low stability and is difficult to use for continuous *in-situ* monitoring [10], while the neutron scattering method uses radioactive samples and in addition to this causing safety concerns, errors can often

This work was supported in part by the Key Project of Natural Science Foundation of Shandong Province of China under Grant ZR2020KC012, in part by the Natural Science Youth Foundation of Shandong Province of China under Grant ZR2020QF088, and in part by the University and Research Institution Innovation Team Program of Jinan under Grant 2020GXRC032 and Grant 2021GXRC037.

Jiamin Wang, Jiqiang Wang, Zhen Li, Zikun Yu, Shuo Li, and Tongyu Liu are with the Laser Institute, Qilu University of Technology (Shandong Academy of Sciences), Jinan, Shandong 250316, China (e-mail: wjm63678537@126.com; jiqiang.wang@sdlaser.cn; zhen.li@sdlaser.cn; 9935909005@qq.com; lsadress@163.com; tongyu.liu@vip.iss-ms.com).

Tong Sun and Kenneth T. V. Grattan are with the Institute of Sensors and Instrumentation, City, University of London, London EC1V 0HB, U.K. (e-mail: t.sun@city.ac.uk; k.t.v.grattan@city.ac.uk).

be seen in the calibration process [11]. Other methods that are used include the Ground Penetrating Radar (GPR) method, which is suitable for moisture content monitoring over large areas, but data received can be difficult to interpret and the results are significantly affected by the ground conductivity [6]. The remote sensing method is mostly used for a macroscopic estimation of the moisture content over a large range, but is not suitable to give accurate measurements when made over a smaller area or with samples of a limited size [12]. This shows that there is an on-going need for new methods to be developed and implemented and optical fiber methods have proved to offer high quality solutions to many other needs in industrial measurement and control.

Optical fiber-based sensing technology shows the outstanding advantages of light weight, corrosion resistance, high intrinsic safety, long transmission distances and easy large-scale networking. In recent years, such sensing techniques have been widely used in the electric power and chemical industries, as well as in mining, in military and security applications and increasingly in other fields [13], [14]. In 2015, Cao *et al.* proposed a distributed measurement method based on carbon fiber heating of an optical cable, where the heating process required an external power supply, with large power consumption seen in an experiment that required a long measurement time [6]. Further, in 2017, Zhu *et al.* have designed a soil moisture sensor using a long-period fiber grating, but the results published showed it was not suitable for measuring low levels of moisture content in a sample [15]. A polymer-coated Fiber Bragg Grating (FBG) sensor has been used for relative humidity sensing [16], but the fabrication of this polymer coating structure is relatively complex and the resulting sensor characteristics are difficult to control. A distributed optical fiber sensor for this type of measurement has been proposed in 2021 by Shi *et al.* – however, an external power supply is also required for this measurement device [17] which can be problematic for its use in some remote locations.

A new approach is proposed here, recognizing the shortcomings of the above (and other) measurement methods, while taking full advantage of the excellent performance of optical fiber-based techniques for different sensing applications. Here the photothermal conversion effect in a doped fiber, combined with the well-established principle of FBG-based temperature measurement, have been combined in an all-fiber moisture content sensor which can provide fast, long distance and on-line monitoring of the moisture content in a range of bulk materials. A further benefit is that it has been designed for in-the-field applications, where conventional power supplies are not available, and thus the low power consumption designed into the sensor system (e.g. from battery use here) is important.

II. Measurement Principle and Structure

A. Principle of All-Fiber Moisture Content Measurement

The measurement approach used in this all-fiber moisture content sensor is discussed below. The key principle is that the different levels of moisture of the sample will lead to the change in its heat conduction performance, as the higher the moisture content, the greater will be its heat conduction capacity [18]. The all-fiber sensing probe with self-heating and temperature measurement functions proposed here has been designed to be inserted into the sample, where the cobalt-doped fiber in the probe allows photothermal conversion from the pump laser energy to thermal energy [19]. The probe temperature can be measured by using the separate FBG-based sensor written into the cobalt-doped fiber [20], and the sample moisture content can be determined, based on a calibration of the relationship between the temperature change which arises due to the heat dissipation by the moisture content [21].

With the reasonable assumption that that the samples considered are homogeneous and isotropic, the internal heat conduction can be modelled as a one-dimensional problem [6]. The quantity of heat generated by the pump laser (per unit length of the doped fiber in unit time) can be given by:

$$Q_1 = k\left|\frac{\mathrm{d}p(l)}{\mathrm{d}l}\right| = k\alpha p_0 e - \alpha l \tag{1}$$

where p_0 is the initial light intensity at the fiber tip containing the FBG, α is the absorption coefficient of the pump laser light in the doped fiber, l is the doped fiber length used and k is the photothermal conversion coefficient (it can be noted that all the above are constants).

The thermal loss therefore is given by:

$$Q_2 = -K\frac{\partial T}{\partial n}\vec{n}_0 \tag{2}$$

where on Eq. (2), K is the thermal conductivity which is related to the nature of matter itself; and $\frac{\partial T}{\partial n}\vec{n}_0$ is the temperature gradient. The thermal energy used to heat the fiber [17], [22] may be expressed as:

$$Q_3 = Q_1 - Q_2 = cm(T - T_0) = cm\Delta T_t \tag{3}$$

where c is the specific heat capacity of the heat source; m is the mass of heat source; T_0 is the initial probe temperature *before* heating; T is the probe temperature *after* heating; and thus $\Delta T_t = T - T_0$ can defined as the temperature difference due to the influence of the moisture present and which indicates the degree of thermal diffusion in the sample, after the initial heating pulse was applied.

The fiber optic temperature sensor approach employed through the doped grating was based on the principle of monitoring the wavelength change of the FBG written into the fiber, from which the probe was constructed, and which is used as the basis of the transducer. Details of the design of such sensors used for temperature measurement (and compensation) have been published elsewhere e.g. [23]–[27]. However, this work takes that design to a different level where, in summary when the grating was subjected to thermal changes due to the presence of the moisture, the temperature change $\Delta T_t = T - T_0$ can then be related to the FBG wavelength shift $\Delta\lambda t$, and this temperature shift is given by

$$\Delta Tt = Kt\Delta\lambda t = Kt(\lambda - \lambda 0) \tag{4}$$

where Kt is the temperature sensitive coefficient of the FBG in the doped fiber. This grating can be used to measure the probe temperature and the temperature change and here $\Delta\lambda t = \lambda - \lambda 0$ indicates the wavelength shift due to the presence of the moisture in the sample. Therefore, the temperature

sensing is undertaken using the FBG-based sensor, which can be characterized by the grating wavelength shift that occurs.

As a result, the thermal conductivity K can be expressed as:

$$K = \frac{cmKt}{\frac{\partial T}{\partial n}\vec{n}_0}(\lambda - \lambda 0) - \frac{k\alpha p_0 e - \alpha l}{\frac{\partial T}{\partial n}\vec{n}_0} \tag{5}$$

When the temperature field is stable and the samples are homogeneous, the temperature gradient $\frac{\partial T}{\partial n}\vec{n}_0$ is constant, and Eq. 5 can be simplified to be as follows:

$$K = k_0 K\mathrm{t}(\lambda - \lambda_0) + b_0 = k_0 \Delta T t + b_0 \tag{6}$$

where $k_0 = \frac{cm}{\frac{\partial T}{\partial n}\vec{n}_0}$, $b_0 = -\frac{k\alpha p_0 e - \alpha l}{\frac{\partial T}{\partial n}\vec{n}_0}$. The sample thermal conductivity, K, is the sum of the liquid thermal conductivity K_w and the solid thermal conductivity $K\mathrm{s}$ (a reasonable assumption is that the gas thermal conductivity can be ignored), and thus:

$$K = K_\mathrm{w} + K_\mathrm{s} \tag{7}$$

When the temperature field is stable, the adjacent solid and liquid matter in the sample are in thermal equilibrium and so their mutual heat transfer can be ignored. There is a positive correlation between K_w and moisture content w, where $K_\mathrm{w} = aw$. As a result, the moisture content of the sample can be given by:

$$w = k_1 \Delta T_t + b_1 \tag{8}$$

where here $k_1 = k_0/a$ is the moisture-temperature conversion coefficient; and $b_1 = -\lambda_s/a + b_0/a$ is the moisture-temperature correction coefficient. It can be seen that there is a linear relationship between the temperature change, ΔT_t and the moisture content w, which then forms the basis of the measurement process in the probe. During the heating process, there is a good (negative) correlation between the probe temperature (characterized by the wavelength shift of FBG) and the moisture content of the sample medium on which the measurement was made. In practice, in this method it can be seen that the higher the moisture content of the sample, the lower is corresponding temperature characteristic change ΔT_t and that their relationship is linear.

B. Design of the All-Fiber Moisture Content Measurement System

The all-fiber moisture content sensing system (as shown schematically in Fig. 1) includes the pump laser source, the sensing probe, a Wavelength Division Multiplexing (WDM) device, a commercial FBG interrogator, and a data processing module. The system used light from the 1480nm pump laser to heat the doped fiber in the sensing probe. The FBG interrogator incorporated a 1550nm pulsed laser (light from which illuminated the FBG used to determine the moisture content) – it also received the reflected signal from this FBG. The WDM in the system was used to combine the pump laser light with the laser light emitted by the interrogator and directed into the probe. Here, the cobalt ion doped into the specialist fiber used absorbed the pump laser energy allowing a photothermal conversion to occur through a non-radiative

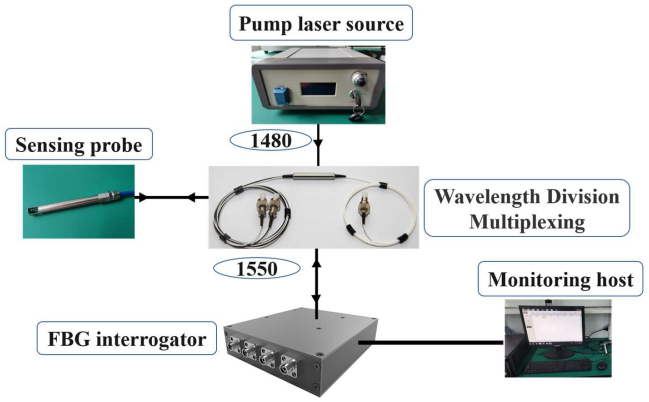

Fig. 1. All-fiber moisture content sensing system design, showing the pump laser source, the FBG interrogator (and monitoring host), the wavelength division multiplexing (at wavelengths shown of 1480 and 1550 nm) and the sensing probe.

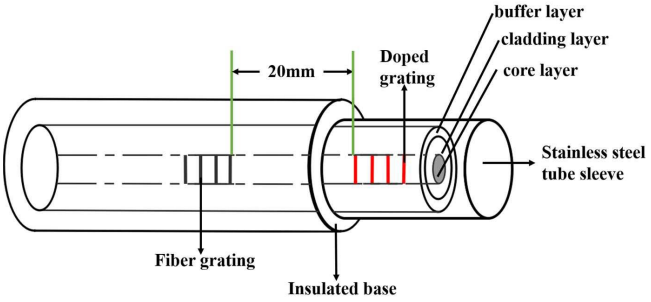

Fig. 2. All-fiber moisture content sensor structure showing the two FBGs used in the system and the insulated base between them.

transition (multi-phonon relaxation). The reflected signal from the FBG, which is characteristic of the temperature change of the probe, entered the interrogator through the WDM module and the wavelength shift was then determined by the calibrated interrogator, allowing the temperature change, ΔT_t to be calculated by the data processing system. This change then could be related to the moisture content, calculated with a knowledge of the linear relationship between the temperature difference ΔT_t and the moisture content (where the relationship is given by Eq. 8).

Fig. 2 shows an illustration of the structure of the all-fiber moisture sensor, showing the two different FBGs used in the system and the insulated base between them. The temperature of the probe will change when inserted into samples with different levels of moisture content, and this results in a shift of the central wavelength of the FBG in the doped fiber, which then can be monitored. In order to eliminate any potential measurement error which would be caused by the environmental temperature changes, a further FBG (the 'compensation grating') was installed (in series with the FBG used for moisture measurement) in the probe itself, to reflect any ambient temperature change of the sample itself (i.e. changes not caused by the moisture effect). In order to reduce any potential measurement error in the reading from this additional FBG which could, for example, be caused by the heat conduction between them, the distance between the two FBGs in the probe used was kept to ~20mm (as shown in Fig. 2). Additionally, as can be seen, a heat insulation base

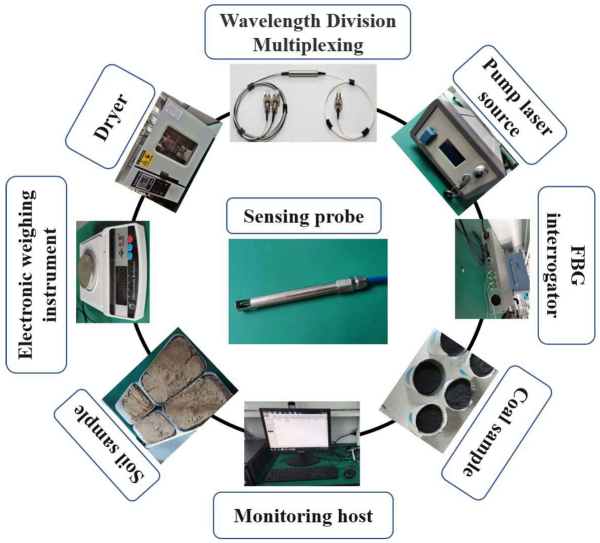

Fig. 3. Basic configuration of test platform, showing the key elements of the device.

was added to limit the heat conduction between the two FBGs used in the probe.

III. Moisture Content Test Platform

To verify the performance of the sensing system designed, and discusssed above, a moisture content test platform was established, as shown schematically in Fig. 3, and used to calibrate the system. This figure illustrates the basic configuration of the test platform – it incorporates an all-fiber moisture content measurement system, the different samples evaluated (e.g. soil, pulverized coal, etc), a dryer, an electronic weighing instrument and other relevant electronic components. The technical specifications of each of the elements of the system are given in Table I.

IV. Experimental Verification of the Sensor System

A. Verification of the Measuring Principles

To evaluate the performance of the sensor system designed in several different situations, five sample groups were studied. There were: sand with a dry density of 1.03g/cm^3 (where the thermal conductivity of bulk materials is mainly related to the moisture content and its density when dry) and the saturated moisture content of 23.87%, samples of anthracite pulverized coal with a dry density of 1.21g/cm^3 and a saturated moisture content of 35.56%, but tested with different moisture contents. These were used with the all-fiber sensing probe discussed above being embedded in the different samples (each sample being of 400g), with these tests being done one-by-one. The pump power from the laser which created the initial probe heating was set to 250mW (to heat the sensor probe directly), as a result of which the wavelength shift of the FBG, previously calibrated for moisture content determination, was measured. In the tests carried out, a sampling point was obtained every second, with an overall experimental monitoring time of 20s being found to allow for a stable measurement to be made.

TABLE I
Components of the Moisture Content Test Platform

Parameter	Value
Soil type	sandy soil
Types of pulverized coal	anthracite
Pump laser source wavelength	1480nm
Demodulator model	GC-97001C
Pump power	≤400mW
Electronic weighing instrument accuracy	0.001g
Drying box temperature/heating time	115℃/12h/5h
Doped FBG center wavelength	1550.038nm
Temperature measuring FBG center wavelength	1539.870nm
Doped fiber length/Pump laser absorption rate	8mm/38%

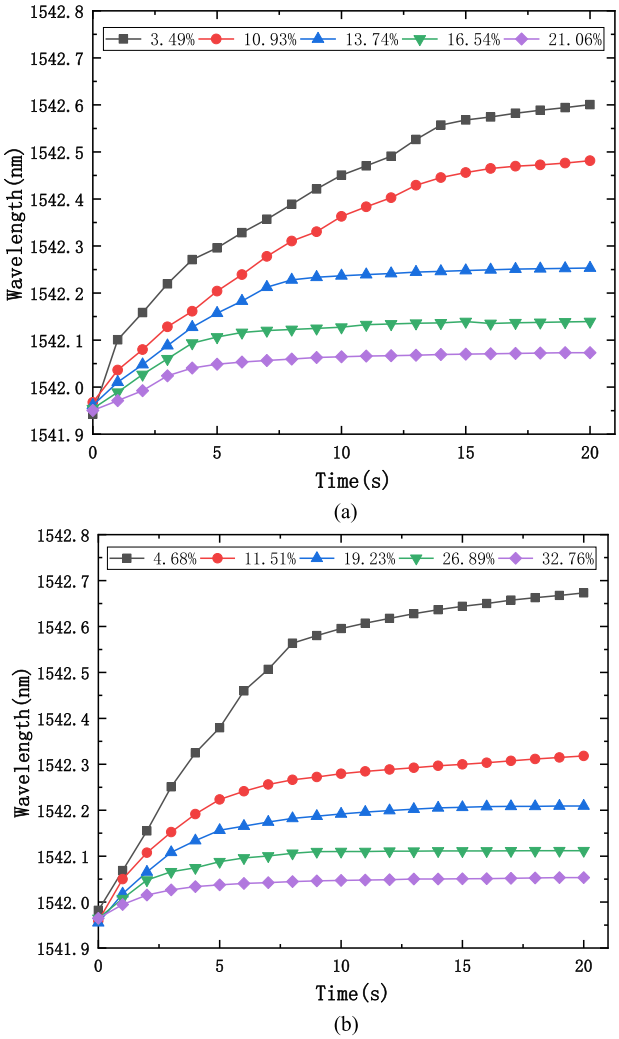

Fig. 4. (a) FBG wavelength shift vs. heating time (in a sandy soil sample of different moisture content values, as shown).(b) FBG wavelength shift vs. heating time (in a pulverized coal sample with diferent moisture content values, as shown).

Fig. 4 shows the wavelength shift of the moisture-monitoring FBG, as a function of the heating time used, when exposed to soil and pulverized coal, each with different levels of moisture content. It can be seen that the probe temperature change (related then to the FBG wavelength shift used for moisture determination) in these different samples (with, as noted different moisture contents) have an upward

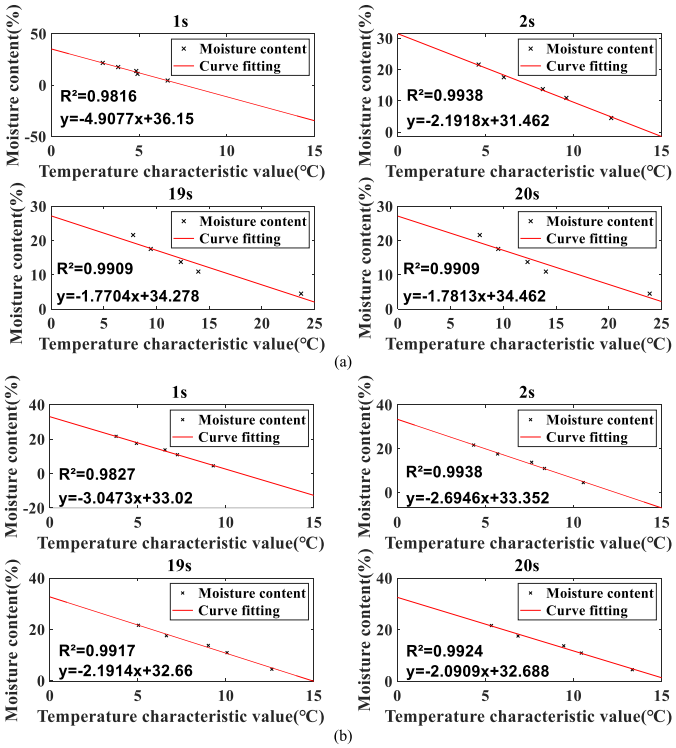

Fig. 5. (a) Fitting between temperature characteristic value and moisture content (in a sandy soil sample) for time periods 1s, 2s, 19s and 20s. (b) Fitting between temperature characteristic value and moisture content (in a pulverized coal sample) for time periods 1s, 2s, 19s and 20s.

trend, with time, after heating was applied. The profile shows that the wavelength shift increases rapidly in the first few seconds, and then the rate of increase of the wavelength change reduces gradually. The higher the moisture content of the sample under evaluation, the smaller is the rate of increase of the wavelength shift. Importantly, the wavelength shift can be seen to positively correlate with the temperature change (reflected in the wavelength change seen for the FBG). It can be seen that the higher the moisture content of the sample surrounding medium, the lower is the temperature change characteristic.

B. Analysis and Verification of the Rapid Measurement

Based on the above testing and calibration of the sensor system, measuring the temperature characteristic value ΔT_t through the all-fiber moisture content monitoring system, and calibrating to show the linear function relationship seen between the temperature characteristic value and the known moisture content, further tests were carried out. In these, different time periods of 1s, 2s, 19s and 20s were selected and then fitted to the temperature characteristic changes of the different soil and pulverized coal samples (each with its corresponding moisture content), to allow the set of calibration graphs shown in Fig. 5 to be determined. It can be seen from the graphs in the figure that for the different substances evaluated, a linear relationship exists between the moisture content and the temperature characteristic (for each specific time period used). Further, the temperature characteristic value decreases with the increase of the sample moisture content.

TABLE II

(A) Comparison of Measurement Error in Soil Moisture Content – Results From All-Fiber Method Compared to Drying Method (%).(B) Comparison of Measurement Error in Pulverized Coal Moisture Content – Results From All-Fiber Method Compared to Drying Method (%)

Drying method	Fiber Method(2s)	Relative Error	Fiber Method(20s)	Error
3.49	4.55	-1.06	1.98	1.51
10.93	10.44	0.49	11.82	-0.89
13.74	13.38	0.36	14.86	-1.12
16.54	17.26	-0.72	17.63	-1.09
21.06	21.38	-0.32	19.98	1.08

(A)

Drying method	Fiber Method(2s)	Error	Fiber Method(20s)	Error
4.68	3.85	0.83	3.80	0.88
14.51	15.13	-0.62	13.61	0.90
21.23	20.86	0.37	22.32	-1.09
30.89	29.76	1.13	31.87	-0.98
32.76	33.23	-0.47	33.77	-1.01

(B)

Additionally, it can be seen that the temperature characteristic value fitting curve (for a specific time period) shows an excellent correlation. Of the different time values used, as would be expected, the graph for the time period of 1s has the smallest fitting coefficient (because the temperature field around the probe is unstable when heating is just started (over that period) and equilibrium has not been reached) while the optimum fitting coefficient was 0.9938 (for the time period of 2s). This outcome shows that the measurement result for a time period of 2s gives both an accurate result and conveniently a fast measurement of the sample moisture content.

C. Measurement Accuracy and Error Analysis

To evaluate the accuracy of the fast response, all-fiber moisture content monitoring system, the different moisture contents of 5 sample groups – these being sandy soil and anthracite pulverized coal (with the same particle diameter) – were determined. Table II shows the result of a comparison of the moisture content determined using the drying method and the All-Fiber Method, with the relative error being determined by the diffference in the two values. The data obtained using the drying method were taken as the benchmark, and when these were compared with the results obtained from the use of the probe reported here, the maximum error of the all-fiber method (for the time period of 2s) was found to be 1.13%, (which is slightly better than that obtained with a time period of 20s). This shows that with a time period of 2s, the advantages of both a high accuracy and a rapid response are realized. These conditions make the sensor system able to make a rapid measurement of moisture content and thus be well suited to many industrial applications, such as model tests in geotechnical engineering, agricultural precision irrigation, and industrial safety, for example.

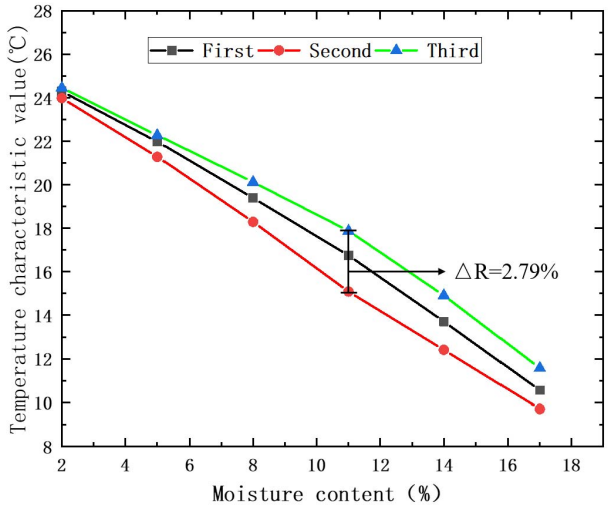

Fig. 6. Repeatability verification of the all-fiber moisture sensor (evaluated in a sandy soil sample).

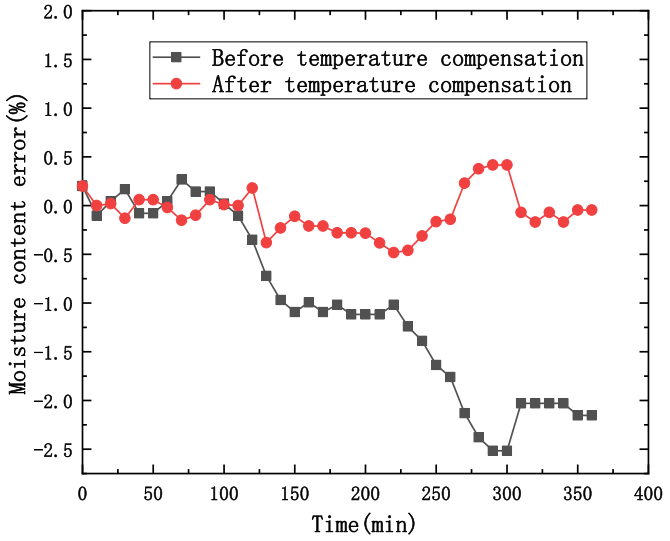

Fig. 7. Comparison of the measurement error (evaluating soil moisture content) before (black dots and line) and after (red dots and line) temperature compensation was applied.

D. Verification of the Repeatability of the Measurements

To evaluate the repeatability of the performance of the all-fiber moisture sensor, six sandy soil samples with different values of moisture content, but esssentially the same diameter and dry density, were selected. The same probe was embedded in these samples in turn, and the temperature characteristic values determined using the sensor probe were measured for a time period of 2s after the start of heating. Then the above process was repeated three times, with the result obtained as shown in Fig. 6. The deviation of the results obtained from the sensor when comparing these three measurements was obtained to be 2.79%, showing the excellent stability of the device. It can be seen that the sensor system maintains a stable performance, with high accuracy in the output.

E. Verification of Ambient Temperature Compensation

Recognizing that there could be some influence on the measurement from changes in the ambient temperature, an experiment has been carried out to investigate the effectiveness of the compensation mechanism, using the second FBG built into the sensor, as shown in Fig. 2. To do this, the probe designed in this work was placed in a sandy soil sample (with a moisture content of 21.3% determined by the drying method) and the values obtained for the moisture content value were recorded every 10min, over an experimental period of 6h, during which a large temperature difference occurred. Fig. 7 shows the results of this experiment, where the moisture content measurement, both with and *without* the temperature compensation being applied were recorded. It can be seen that the change of ambient temperature had an impact on the reading from the output of the sensor – without the temperature compensation being applied, the maximum error reached -2.51%. However, after temperature compensation (using data from the reference grating built into the probe) was applied, the error was significantly reduced to be within ±0.5%. In this way, the influence of diurnal temperature variations or seasonal changes on the measurement results can be eliminated very effectively when the probe is in use.

V. Conclusion

In this work, a new design of an all-fiber moisture sensor showing a fast response has been developed, using a new technique which adopts a doped optical fiber as a heating element with a FBG inscribed in the fiber as the primary temperature measuring element. The sensor has been designed to work well even when the ambient temperature changes and corrections for ambient temperature changes were applied using data from a nearby 'comensation grating' built into the probe. The design, fabrication and feasibility of this innovative approach have been described and the device performance validated through a series of moisture content measurements on a range of different types of samples. The stability and accuracy of the sensor system were further verified through a series of experiments carried out, using a special moisture content test platform and samples of different types and humidity level (calibrated against the 'gold standard' benchmark drying method). The results of this series of experiments carried out in these different media show that the sensor developed was capable of making measurements within a short time period of ∼2s while at the same time the maximum error in the humidity measurement is just over 1%. This novel detection system has been show to be capable of measuring humidity changes in many different types of samples, these varying from different soils to pulverized coal and showing the wide potential of the method for monitoring moisture levels in a range of different types of samples. Further, the method is intrinsically safe as, being all-optical at the sensor probe, it does not need an external power supply as there are no currents flowing at the sensor probe. In that way it can be used safely in mining applications or in biodigesters or sewers, for example [25], [26] (where explosive gases such as methane are present), taking advantage of the fast measurement speed and probe temperature compensation integrated into the probe design.

Acknowledgment

Support from the Royal Academy of Engineering and the George Daniels Educational Trust is greatly appreciated.

REFERENCES

[1] B. Zhao *et al.*, "Estimation of soil moisture using modified antecedent precipitation index with application in landslide predictions," *Landslides*, vol. 16, no. 12, pp. 2381–2393, 2019.

[2] E. R. Sujatha and V. Sridhar, "Mapping debris flow susceptibility using analytical network process in Kodaikkanal hills, Tamil Nadu (India)," *J. Earth Syst. Sci.*, vol. 126, no. 8, p. 116, Dec. 2017.

[3] D. C. Mason, J. Garcia-Pintado, H. L. Cloke, and S. L. Dance, "Evidence of a topographic signal in surface soil moisture derived from ENVISAT ASAR wide swath data," *Int. J. Appl. Earth Observ. Geoinf.*, vol. 45, pp. 178–186, Mar. 2016.

[4] R. Arezou, P. Maria, and R. Mehrdad, "Assessment of soil moisture content measurement methods: Conventional laboratory oven versus halogen moisture analyzer," *J. Soil Water Sci.*, vol. 4, no. 1, pp. 151–160, Dec. 2020.

[5] V. Radman and M. Radonjic, "Arduino-based system for soil moisture measurement," in *Proc. 22nd Conf. Inf. Technol. (IT)*, 2017, pp. 289–292.

[6] D. Cao, B. Shi, H. Zhu, G. Wei, S.-E. Chen, and J. Yan, "A distributed measurement method for *in-situ* soil moisture content by using carbon-fiber heated cable," *J. Rock Mech. Geotech. Eng.*, vol. 7, no. 6, pp. 700–707, Dec. 2015.

[7] C. Liang, X. Chen, C. Zhao, W. Pu, P. Lu, and C. Fan, "Flow characteristics and dynamic behavior of dense-phase pneumatic conveying of pulverized coal with variable moisture content at high pressure," *Korean J. Chem. Eng.*, vol. 26, no. 3, pp. 867–873, May 2009.

[8] Y.-C. Chen, H.-C. Yeh, M.-W. Gui, C. Wei, and C.-H. He, "Estimation of surface soil moisture content using fractals," *Environ. Monitor. Assessment*, vol. 193, no. 2, pp. 1–11, Feb. 2021.

[9] D. J. Kim, S. I. Choi, O. Ryszard, J. Feyen, and H. S. Kim, "Determination of moisture content in a deformable soil using time-domain reflectometry (TDR)," *Eur. J. Soil Sci.*, vol. 51, no. 1, pp. 119–127, Mar. 2000.

[10] F. Rahimi-Ajdadi, Y. Abbaspour-Gilandeh, K. Mollazade, and R. P. R. Hasanzadeh, "Development of a novel machine vision procedure for rapid and non-contact measurement of soil moisture content," *Measurement*, vol. 121, pp. 179–189, Jun. 2018.

[11] A. E. Badr and M. E. Abuarab, "Soil moisture distribution patterns under surface and subsurface drip irrigation systems in sandy soil using neutron scattering technique," *Irrigation Sci.*, vol. 31, no. 3, pp. 317–332, May 2013.

[12] X. Zhang, C. Yang, and L. Wang, "Research and application of a new soil moisture sensor," in *Proc. MATEC Web Conf.*, vol. 175, 2018, p. 02010.

[13] J. S. Hallett *et al.*, "Soil moisture content measurement using optical fiber long period gratings," in *Proc. 25th Opt. Fiber Sensors Conf. (OFS)*, Apr. 2017, pp. 1–4.

[14] Z. Song, B. Shi, H. Juang, M. Shen, and H. Zhu, "Soil strain-field and stability analysis of cut slope based on optical fiber measurement," *Bull. Eng. Geol. Environ.*, vol. 76, no. 3, pp. 937–946, Aug. 2017.

[15] H.-H. Zhu, B. Shi, J. Zhang, J.-F. Yan, and C.-C. Zhang, "Distributed fiber optic monitoring and stability analysis of a model slope under surcharge loading," *J. Mountain Sci.*, vol. 11, no. 4, pp. 979–989, 2014.

[16] T. L. Yeo, T. Sun, K. T. V. Grattan, D. Parry, R. Lade, and B. D. Powell, "Characterisation of a polymer-coated fibre Bragg grating sensor for relative humidity sensing," *Sens. Actuators B, Chem.*, vol. 110, no. 1, pp. 148–156, Sep. 2005.

[17] B. Shi *et al.*, "DFOS applications to geo-engineering monitoring," *Photonic Sensors*, vol. 11, no. 2, pp. 158–186, Jun. 2021.

[18] J. Ren, L. Men, W. Zhang, and J. Yang, "A new empirical model for the estimation of soil thermal conductivity," *Environ. Earth Sci.*, vol. 78, no. 12, p. 361, Jun. 2019.

[19] M. K. Davis, M. J. F. Digonnet, and R. H. Pantell, "Thermal effects in doped fibers," *J. Lightw. Technol.*, vol. 16, no. 6, pp. 1013–1023, Jun. 1, 1998.

[20] D. Junwei, L. Weiping, T. Cui, and Y. Xida, "Fire detector based on serial FBG temperature sensors optical cabling," *J. Phys., Conf. Ser.*, vol. 1550, no. 4, May 2020, Art. no. 042054.

[21] J. M. Wang, Z. Li, and J. Q. Wang, "All-optical fiber miniature soil moisture content sensor," *Infr. Laser Eng.*, vol. 51, no. 3, pp. 1–6, 2021. [Online]. Available: http://hp.kn cnki.net.qlu.vpn358.com/kcms detail/12.1261.tn.20210916.1447.006.html

[22] D. F. Cao, S. Bin, and J. F. Yan, "Based on the C—DTS soil moisture content distributed measurement method research," *Chin. J. Geotech. Eng.*, vol. 36, no. 5, pp. 910–915, 2014.

[23] K. T. V. Grattan and B. T. Meggitt, *Optical Fiber Sensor Technology*, vol. 2. London, U.K.: Chapman & Hall, 1998.

[24] K. T. V. Grattan and B. T. Meggitt, *Optical Fiber Sensor Technology*, vols. 3–4. Boston, MA, USA: Academic, Boston, MA, USA, 1999.

[25] L. Alwis, T. Sun, and K. T. V. Grattan, "Developments in optical fibre sensors for industrial applications," *Opt. Laser Technol.*, vol. 78, pp. 62–66, Apr. 2016.

[26] B. Rente *et al.*, "A fiber Bragg grating (FBG)-based sensor system for anaerobic biodigester humidity monitoring," *IEEE Sensors J.*, vol. 21, no. 2, pp. 1540–1547, Jan. 2021.

[27] B. Rente *et al.*, "Extended study of fiber optic-based humidity sensing system performance for sewer network condition monitoring," *IEEE Sensors J.*, vol. 21, no. 6, pp. 7665–7671, Mar. 2021.